Study on Distribution Characteristics of Gas-Liquid Two-Phase Flow in Pitot tube Sampler

Study on Distribution Characteristics of Gas-Liquid Two-Phase Flow in Pitot tube Sampler

Miao Yang[1*], ZhiAn Deng[1], ZhiBo Cao[2], Jun Li[2], Zi Yan Wen[1]

[1]Author address: College of Petroleum Engineering, Xi'an Shiyou University, Xi'an 710065, China
[2]Author address: Xinjiang Oilfield Company, 834000, China

*Corresponding author's e-mail: 1169004952@qq.com

Abstract. Gas-liquid two-phase current systems are widely existed in the petroleum, the chemical industry, the metallurgy, the nuclear power and many industrial fields. Two-phase's phase distribution and measurement can't be avoided in two phase current system. And it is also a difficult problem that has not been solved. In this paper, we designed a pitot-distributor. Experimental measurement and theory analysis were carried out to study the distribution data and situation of the distributor in gas-liquid two-phase flow. Firstly, a special experimental device for pitot-distributor was designed and experiments were carried out at air-water two-phase flow loop. The main text pipeline's diameter is 50mm, the system pressure is 0.24~0.28MPa, there are five branches in the pitot-distributor, each branch's diameter is 8mm. The paper has first analyzed the influencing factors of gas extraction ratios and liquid extraction ratios, which were effected by four different types of pitot-separator. Next, it analyzed different efforts under two kind of pressure. Then, we established the math model and calculated the coefficients. Last, we analyzed the erroneous.The experimental result indicated that the tube-12345 structure is the perfect one which can keep extraction ratios more stable in a quite wide rang. Liquid extraction ratios (K_L) mainly are affecting by the pressure and its structure. The gas extraction ratios (K_G) mainly are affecting by the pressure.

1. Analysis of Distribution Characteristics of Pitot Tube Sampler

1.1. Pitot sampler structure

The pitot tube sampler designed in this paper can transform four different sampling structures by opening or closing the ball valve. The sampling sections are shown in Figure 1-1a, 1-1b, 1-1c and 1-1d, which are represented as "branch tube-12345", "branch tube-234", "branch tube-1234" and "branch tube-2345" respectively. Table 1-1 lists the four types of Pitot sampler size data.

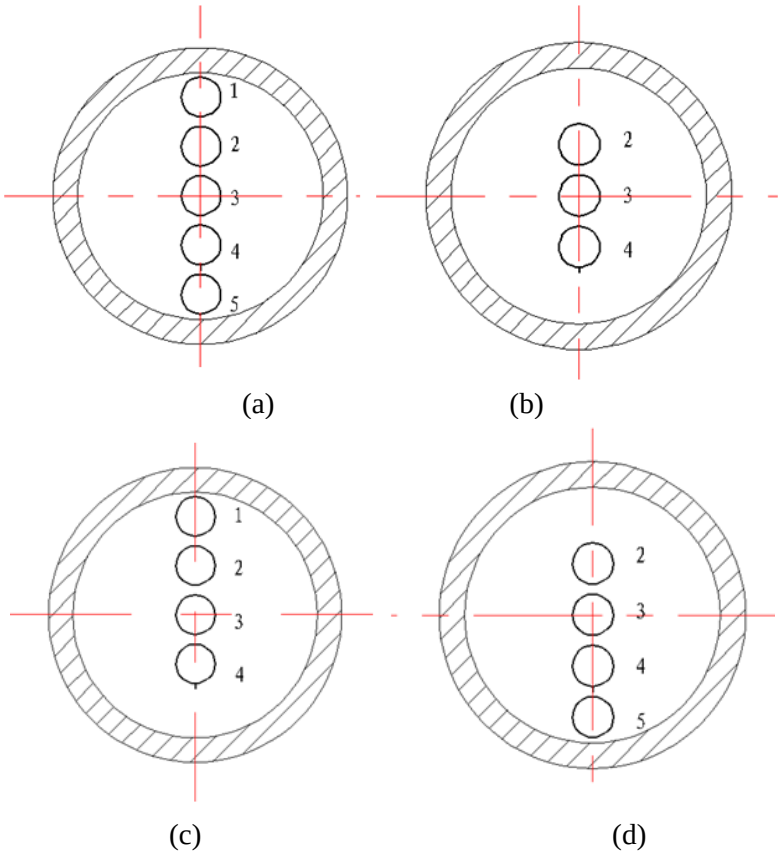

Figure 1-1 Schematic diagram of four pitot tube samplers

Table 1-1 Sampler structure data

Sample tube model	Number of branches	Sampling diameter(mm)	Port area(mm^2)	Total circulation area(mm^2)	Percentage of total cross-sectional area (%)
branch tube-12345	5	8	50.3	251.2	12.8
branch tube-234	3	8	50.3	150.8	7.68
branch tube-1234	4	8	50.3	201.1	10.24
branch tube-2345	4	8	50.3	201.1	10.24

Table 1-2 shows the experimental industrial and mining table. In the experiment, two pressures of 0.24 MPa and 0.29 MPa are set under each gas-liquid flow rate. The high pressure is basically close to the highest value that the experimental device can withstand. The difference between the two pressures is about 0.05 MPa.

1.2. Analysis of the splitting coefficient of different pitot tube samplers

1.2.1. Influence of pitot tube structure on liquid phase splitting coefficient

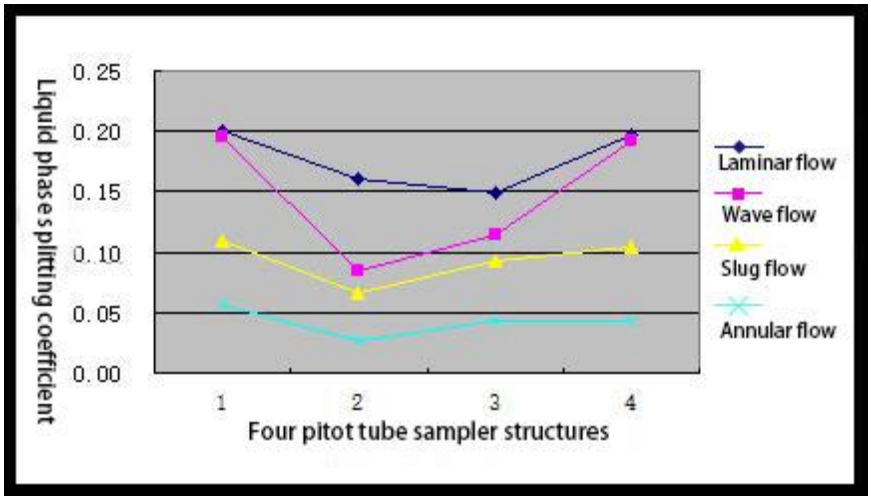

Figure 1-2 an Actual measurement of liquid phase splitting coefficient under four pitot tube sampler structures (I)

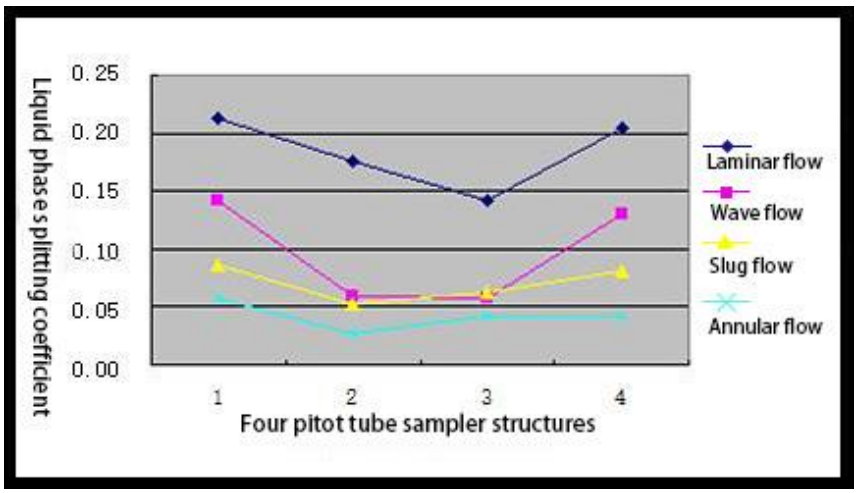

Figure 1-2 b Actual measurement of liquid phase splitting coefficient under four pitot tube sampler structures (II)

Figure 1-2 shows the liquid phase splitting coefficients of the four pitot tube samplers. The X-axis is the four pitot tube sampler structures. 1, 2, 3 and 4 represent tube-12345, tube-234, tube-1234, tube-2345, respectively, and the ordinate is the liquid phase split coefficient, now analyze Figure 1-2:

When the laminar flow, the gas-liquid flow rate is slow, the liquid phase is mainly in the lower part of the pipeline due to gravity, and the uppermost branch tube 1 can hardly receive liquid, so the tube-12345 is basically the same as the tube-2345 (1, 4), the tube-234 and the tube-1234 is basically the same (2, 3), and when the same four branches, the tube-2345 has a larger split coefficient than the tube-1234. Comparing Figure 1-2 a and b, it can be seen that the pressure has little effect on K_L, and the liquid phase split coefficient under laminar flow mainly depends on the position of the branch pipe in the cross section.

There is no absolute division criterion for wave flow and laminar flow. The two flow patterns are also classified as wave laminar flow when dividing the flow pattern. Therefore, similar to laminar flow, the upper part of the pipe is gas and the lower part is liquid. Therefore, tube-12345 is basically the same as tube-2345; wave flow is different from laminar flow in that the flow pattern has volatility, and the gas-liquid interface is wavy line, so even in a relatively stable flow pattern (assuming that the gas content of the cross section is equal to the liquid content of the cross section), the sample bodies of the branch tubes 1, 2, and 3 may be a gas-liquid mixture. Therefore, the shunt coefficient of tube-12345 is greater than tube-2345 and tube-234, and tube-12345 is slightly larger than tube-2345. The tube-2345, which is also the same, has a larger split coefficient than the tube-1234. Comparing Figure 1-2a and b, it can be seen that the pressure has an influence on K_L, the greater the pressure, the greater the volatility of the wave current and the slightly different shunt coefficients.

Slug flow is an intermittent flow in which long bubbles and liquid plugs alternately flow through the distribution tube section. Taitel et al. suggest that the flow structure of the slug flow can be simplified to a unit body composed of long bubbles and liquid plugs. The distribution under the slug flow can be seen as a superposition of the two parts of the liquid membrane zone distribution and the liquid plug zone distribution. When there is no liquid plug, similar to the laminar flow condition, when the liquid plug comes, the pressure in the distribution pipe suddenly increases, and the spoiler installed in front of the sampling distributor rotates to form a symmetrical annular flow. Therefore, branch tube-12345 has the largest liquid phase split coefficient, tube-234 is the least, and tube-2345 is larger than tube-1234 because of the similar laminar flow when there is no liquid plug. Comparing Figures 1-2 a and b, it can be seen that the pressure has an effect on K_L, the greater the pressure, the smaller the shunt coefficient. Basically, under the pressure of 1 industrial and mining, the liquid phase splitting coefficient is proportional to the branch pipe occupying the cross-sectional area of the pipe.

In the case of annular flow, the amount of liquid is very small, the middle three branches are located in the gas concentration area, and the upper and lower branches are facing the annular liquid film. As can be seen from the figure, the tube-1234 is slightly larger than the tube-2345, this is because the liquid film is uneven and the lower liquid film is thick. Tube-234 is located in the gas concentration zone, the amount of liquid taken is very small, and the value of the shunt coefficient of tube-12345 is the largest. Comparing Figure 1-2 a and b, it can be seen that the pressure has little effect on K_L, because the pressure of the annular flow itself is very large, and the difference of 0.05MPa is not obvious.

1.2.2. Influence of pitot tube structure on gas phase splitting coefficient. Figure 1-2 shows the gas phase splitting coefficient of the four pitot tube samplers. The X axis is the four pitot tube sampler structures. 1, 2, 3 and 4 represent tube-12345, tube-234, tube-1234, tube-2345, respectively, and the ordinate is the gas phase splitting coefficient. Now analyze Figure 1-2:

In the laminar flow, the gas phase splitting coefficient is stable under the structure of the four pitot tube samplers. This is because the gas phase and the liquid phase have obvious boundaries when laminar flow, so the tube-12345 and tube-1234 structures in the gas concentration zone have many branches. The gas is the most, the tube-1234 split coefficient is larger; The wave flow is similar to the laminar flow, but due to the large fluctuation of the wave flow, when the gas slug flow is also carried in the branch tube located in the liquid concentration zone, the gas phase split coefficient of the tube-1234 is the largest; In the case of slug flow, when there is no liquid plug, similar to the laminar flow and the wave flow, the gas is mainly obtained in the gas concentration zone, and when the liquid plug is present, the pressure inside the tube increases to cause the spoiler to rotate (see the first section of Chapter 4). Forming an annular flow, the intermediate gas concentration zone can take gas. In the upper and lower liquid concentration zone, since the liquid film thickness is smaller than the inner diameter of the sampling tube, the gas-liquid mixture can also be obtained, and the pipe-12345 takes the most gas; In the case of annular flow, the gas-phase splitting coefficients of the other four structures are the most stable except for tube-12345, which is maintained between 0.04 and 0.05.

Comparing Figure 1-3 a and b, it can be seen that the pressure has an influence on the gas phase shunt coefficient. The larger the pressure, the more gas is taken, and the shunt coefficient is larger.

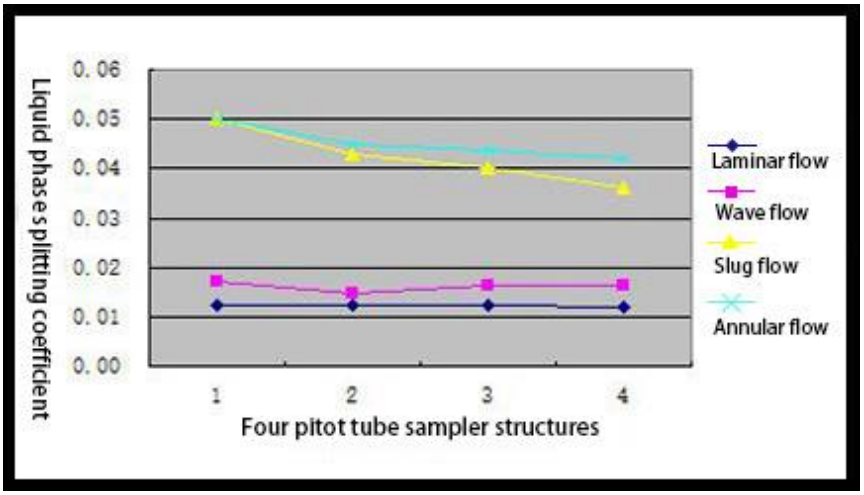

Figure 1-3 a Real-time measurement of gas phase shunt coefficient under four pitot tube sampler structures (I)

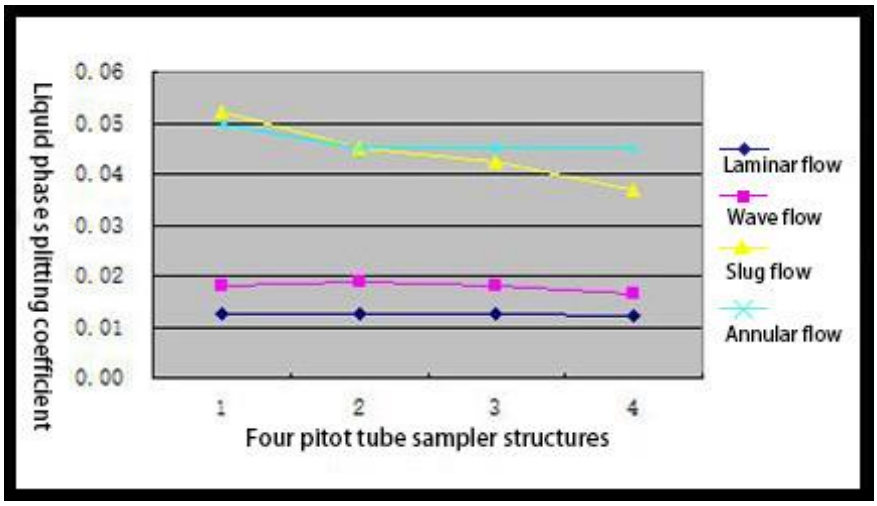

Figure 1-3 b Actual measurement of gas phase splitting coefficient under four pitot tube sampler structures (II)

Table 1-2 shows the comparison of the four structures and sampling characteristics of the pitot tube sampler. For the tube-12345 type with evenly distributed branch pipes, it can be ensured that the branch pipes are located in the gas phase concentration zone and the liquid phase concentration zone simultaneously in each flow mode, and the split fluid entering the split circuit has both gas and single phase liquid, or a two-phase fluid having a constant gas-bearing gas rate. The sampling representative can be improved by using a plurality of sampling branches to uniformly distribute the sampling in the main section. However, the volatility of different flow patterns is very different and cannot be generalized. It requires a split-type discussion (see Chapter 4). However, it can be determined that under the two flow patterns of laminar flow and wave flow, the gas phase split coefficient is not affected by the sampling tube distribution.

Table 1-2 Dispenser structure and sampling characteristics

Distributor name	Schematic	Sampling position and structural characteristics	Sampling characteristics
Tube-12345	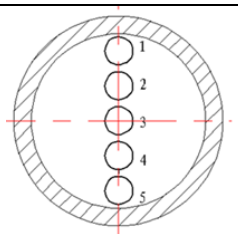	The branch tube is evenly distributed throughout the main section	Uniform sampling and large shunt coefficient
Tube-234	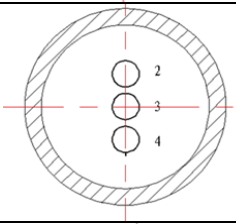	Branch tubes are distributed in the central area of the competent authority	Uniform sampling, small splitting coefficient (larger annular gas phase split)
Tube-1234	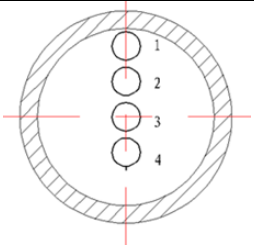	Branch tube biased to gas concentration zone	The sampling results are affected by the flow pattern, ie the gas-liquid phase distribution
Tube-2345	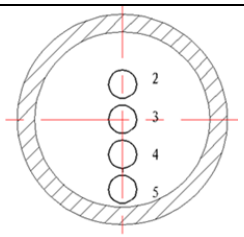	Branch tube biased to liquid concentration zone	The sampling results are affected by the flow pattern, ie the gas-liquid phase distribution

1.3. Influence of flow on shunt coefficient

Table 1-3 Experimental condition table

Air flow volume / Water flow volume	300	500	800	1000	1500	2000	5000
12	√	√	√	√		√	√
20	√	√	√	√		√	√
35		√	√	√			
45				√	√		

Table 1-3 shows the gas phase and liquid phase volume flow in the main road in the experiment. Since the tube-12345 takes more gas and liquid phase and is uniform, therefore, tube-12345 is taken as an example to study the effect of gas/liquid flow on the splitting coefficient.

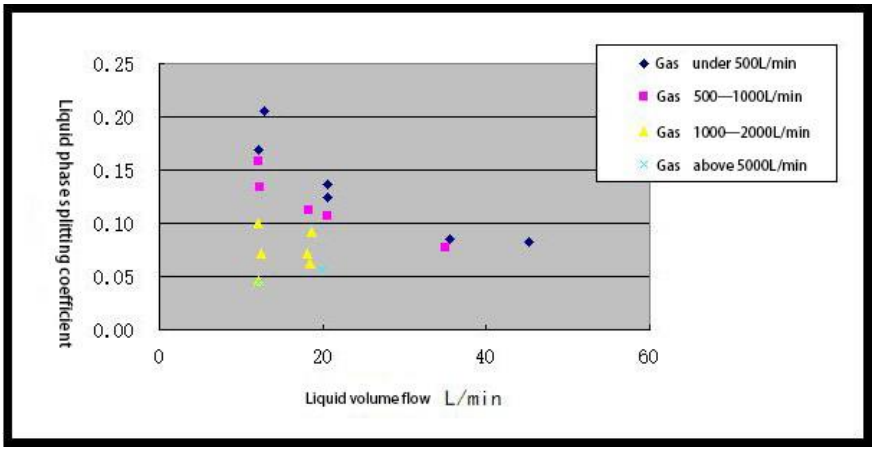

Figure 1-4a Actual measurement of liquid phase split coefficient with liquid volume flow

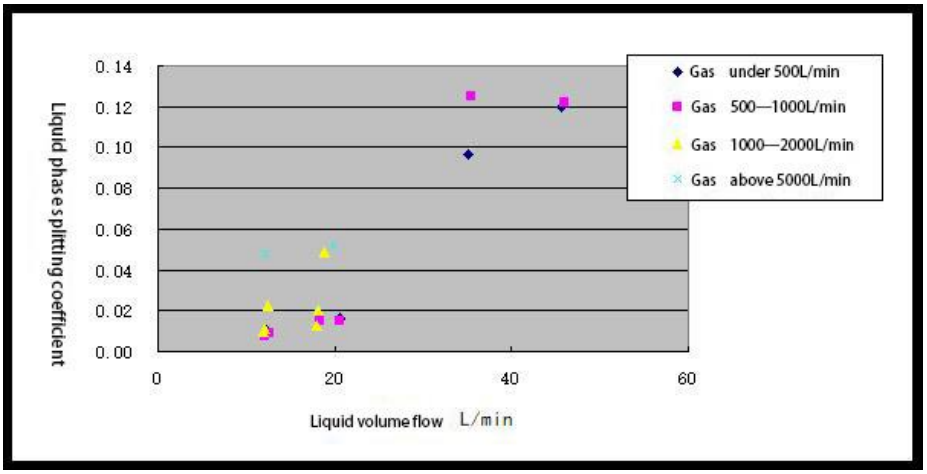

Figure 1-4b Actual measurement of gas phase splitting coefficient with liquid volume flow

It can be seen from the analysis of Figure 1-4 that the liquid-phase splitting coefficient decreases with the increase of the liquid volume flow rate, and the larger the flow rate, the more the liquid is taken; the gas-phase splitting coefficient increases with the increase of the liquid volume flow rate, but the change is not obvious. This is due to the different volatility of different flow patterns, and also requires split analysis.

It can be seen from the analysis of Figure 1-5 that the liquid phase splitting coefficient decreases with the increase of gas volume flow rate, and the larger the gas volume is, the smaller the liquid is taken; the gas phase splitting coefficient is not obvious with the increase of gas volume flow.

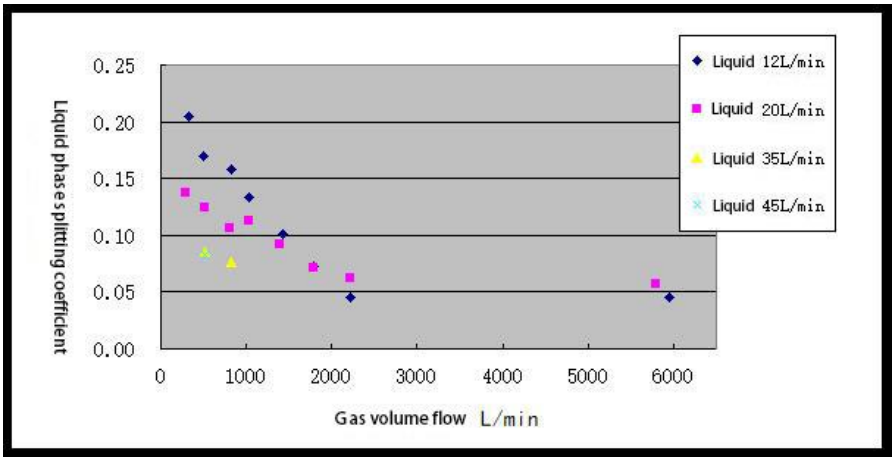

Figure 1-5a Actual measurement of liquid phase split coefficient with gas volume flow

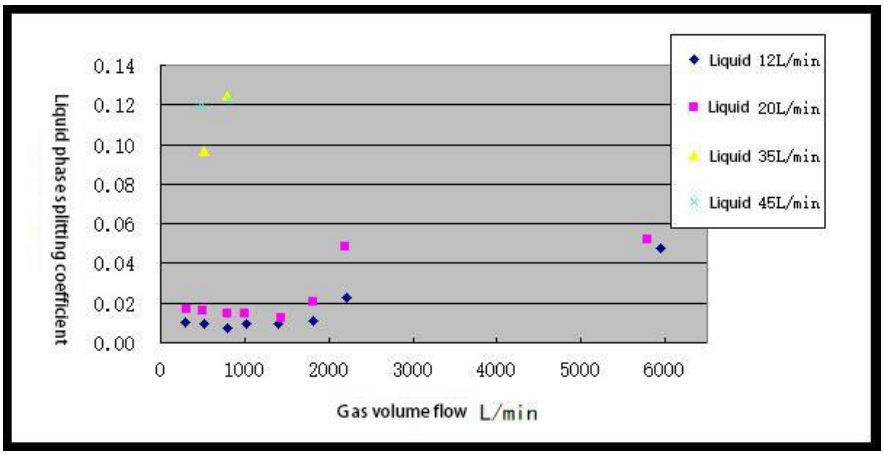

Figure 1-5b Actual measurement of gas phase splitting coefficient with gas volume flow

When the gas-liquid two-phase fluid flows in the pipeline, various flow structure forms will be traveled due to different pressure, flow, heat load and pipe geometry, which is referred to as flow pattern. The more common horizontal flow patterns currently recognized include stratified flow, wave flow, slug flow, bubble flow, annular flow and the like. Since different gas-liquid two-phase flow patterns have different hydrodynamic and heat transfer characteristics [17], it is necessary to divide the flow pattern to study the flow pattern control when studying the gas-liquid two-phase flow problem. Here, do not make more statements.

2. Mathematical model of distribution characteristics of flow-based pitot host sampler

2.1. Establishment of mathematical model

The sample body is in parallel relationship with the main fluid, so the split coefficients K_G, K_L mainly depend on the relative resistance characteristics of the main fluid circuit and the sample body circuit. In addition, the number and position of the sampling tubes also have a large influence on the characteristics of the shunt coefficient. The phase separation model in the two-phase flow theory can be used to write the calculation formula of the total pressure difference ΔP_1 of the main fluid circuit and the total pressure difference ΔP_2 of the sample body loop:

$$\sqrt{\Delta P_1} = \sqrt{\frac{\xi_1}{2\rho_G}}[\frac{(1-k_g)M_G}{A_1}] + \theta_1\sqrt{\frac{\xi_1}{2\rho_l}}[\frac{(1-k_l)M_l}{A_1}] \tag{2-1}$$

$$\sqrt{\Delta P_2} = \sqrt{\frac{\xi_2}{2\rho_G}}\left(\frac{K_G M_G}{A_2}\right) + \theta_2\sqrt{\frac{\xi_2}{2\rho_L}}\left(\frac{K_L M_L}{A_2}\right) \tag{2-2}$$

In the formula, ξ_1 and ξ_2 are the total resistance coefficients of the main fluid circuit and the sample body circuit respectively. ρ_G And ρ_L are the density of the gas phase and the liquid phase, respectively. A2 A3 is the flow cross-sectional area of the main fluid circuit and the sample body circuit respectively, and θ_1 is the primary fluid circuit phase separation model correction coefficient, and θ_2 is the sample body loop phase separation model correction coefficient. In the experiment, the upstream pressure is the mixing pressure, and the final end of the main fluid and the sample body are at atmospheric pressure, so the pressure difference between the two stages is equal, that is, $\Delta P_1=\Delta P_2$, and the following relationship can be derived from the formulas (2-1) and formula (2-2):

$$[1+\sqrt{\frac{\xi_2}{\xi_1}\left(\frac{A_1}{A_2}\right)}]K_G = 1+[\theta_1(1-K_L)-\theta_2\sqrt{\frac{\xi_2}{\xi_1}\left(\frac{A_1}{A_2}\right)}K_L]\sqrt{\frac{\rho_G}{\rho_L}\left(\frac{M_L}{M_G}\right)} \tag{2-3}$$

Equation (2-3) comprehensively reflects the relationship between the gas phase splitting coefficient K_G, the liquid phase splitting coefficient K and the two-phase fluid density, the structural parameters, and the gas phase and liquid phase of the two-phase fluid to be measured. When the gas-liquid two-phase fluid and structural parameters are known, both the gas phase splitting coefficient K_G and the liquid phase splitting coefficient K_L are unknown, and therefore K_G and K_L cannot be obtained according to the formula (2-3). Therefore, it is necessary to add another complementary equation relation about K_G and K_L in order to solve its value. After the summary of the predecessors, it is found that the gas-liquid two-phase fluid can improve the kinetic energy through the flow type intervention, and the liquid film on the wall will be torn and pulverized. As the air flow is dispensed, a small amount of liquid film will also be killed and also low. The spray is told from the mixer mouth, but a small amount of liquid film remains on the wall; the spray from the spoiler tells the droplet that its movement has a certain independence due to inertia and is basically unaffected by the gas phase. Therefore, the liquid phase flow into the sampling tube is equal to the total droplet flow [100] of the cross section of the sampling tube port. This is:

$$M_{L3} = (M_L - \Delta M_{LF})\cdot\alpha = \alpha\cdot M_L - b \tag{2-4}$$

Where ΔM_{LF} represents the residual liquid film flow rate, $b = a\cdot M_{LF}$, a is a coefficient related to the distribution pattern of the droplet on the pipe flow cross section and the sampling tube structure. The calculation formula of the liquid phase split coefficient K_L can be obtained:

$$K_L = \alpha\left(1+\frac{b}{M_{L3}}\right)^{-1} \tag{2-5}$$

It can be seen from equation (2-5) that K_L gradually increases as the liquid sample flow rate increases. When M_{L2} increases to a certain value, the latter phase b/ M_{L3} in parentheses will be small

relative to 1, can be ignored, at this time K_L is equal to the constant a. After determining the liquid phase splitting coefficient, the calculation formula of the gas phase splitting coefficient K_G can be obtained according to the formula (2-3):

$$K_G = K_{G1} + \Delta K_G \tag{2-6}$$

Where K_{G1} is the value of the shunt coefficient when the dryness is equal to 1, and ΔK_G is the influence of K_L and other factors on K_G. Can be calculated separately using the formula below

$$K_G = [1 + \sqrt{\frac{\xi_2}{\xi_1}}\left(\frac{A_1}{A_2}\right)]^{-1} \tag{2-7}$$

$$\Delta K_G = K_{G1}[\theta_1(1 - K_L) - \theta_2\sqrt{\frac{\xi_2}{\xi_1}\left(\frac{A_1}{A_2}\right)K_L}]\sqrt{\frac{\rho_G}{\rho_L}}\left(\frac{M_L}{M_G}\right) \tag{2-8}$$

2.2. Determination of the coefficient of the mathematical model

Equations (2-5) ~ (2-8) are formula models of pitot-type samplers derived from the formula, where the coefficients a, b are unknown and need to be calibrated using measured data.

Table 2-1 lists the range of liquid volume flow and gas volume flow for the four flow patterns studied (laminar, wave, slug, annular). Longitudinal comparison of Figure 2-1 to Figure 2-4, with the increase of gas volume flow, K_L gradually becomes smaller under the four flow patterns of laminar flow, wave flow, slug flow and annular flow, and it can be seen that K_L is greatly affected by the gas flow rate.

According to the empirical formula (2-5), we can see that the liquid phase split coefficient K_L is proportional to the sampled liquid mass flow M_{L3} and tends to be stable with the increase of M_{L3}. Figure 2-1 ~ Figure 2-4 show the measured results of the liquid phase split coefficients of the four flow patterns and the five pitot tube structures. The abscissa in the figure is the liquid phase mass flow M_{L3} of the sample body, and the ordinate is The measured liquid phase split coefficients are (I)(II) for each set of plots for two pressures (0.24 MPA and 0.29 MPA). After observation, the liquid phase splitting coefficient K_L agrees well with the theoretical trend of the empirical formula (2-5).

Figure 2-5 ~ Figure 2-8 show the measured results of the gas phase splitting coefficients of the four flow patterns and the five pitot tube structures. The abscissa in the figure is the liquid phase mass flow M_{L3} of the sample body, and the ordinate is the measured. The gas phase splitting coefficient of each group (I) (II) is a measured map of two pressures (0.24 MPA and 0.29 MPA).

Analysis of Figure 2-5 and Figure 2-6: In the laminar flow and wave flow, under the structure of the four pitot tube samplers, the gas phase splitting coefficient is relatively stable and the value is close; Analysis Figure 2-7: Tube-12345 takes the most gas when slug flow, because the slug flow is a unit body composed of long bubbles and liquid plugs. When there is no liquid plug, it is similar to laminar flow and wave flow. The concentrated area mainly obtains gas. When there is liquid plug, the pressure inside the tube increases to make the spoiler rotate, forming a symmetrical annular flow and the middle gas concentration area can take gas. In the upper and lower liquid concentration area, since the liquid film thickness is smaller than the inner diameter of the sampling tube, obtaining a gas-liquid mixture; Analysis Figure 2-8: The gas phase splitting coefficient is the most stable when the annular flow is used.

Comparing the measured maps under the two pressures in Figure 2-5 ~ Figure 2-8, it can be found that the pressure at the laminar flow has a greater influence on the gas-phase splitting coefficient. The greater the pressure, the more gas is taken. When comparing the flow patterns longitudinally, it can be found that the gas phase splitting coefficient K_G is greatly affected by the liquid phase flow rate, while

the gas phase flow rate (gas phase conversion speed) has little effect on the K_G. ΔK_G is small, K_G and K_{G1} are very close, and the difference between the two is basically not affected by the gas phase flow rate and the liquid phase flow rate.

Table 2-1 Comparison of different types of industrial and mining

Flow pattern	Liquid volume flow(L/min)	Gas volume flow(L/min)	Figure
Laminar flow	12~20	300~800	3 -9
Wave flow	12~20	1000~2000	5-2
Slug flow	35~50	800~1000	5-3
Annular flow	12~20	5000~6000	5-4

According to the measured data map, (based on tube-12345), in Equation 2-5, the values of a and b are shown in Table 2-2.

Table 2-2 Different flow coefficient

Flow pattern / coefficient	Laminar flow	Wave flow	Slug flow	Annular flow
a	0.22	0.2	0.11	—
b	0.73	0.82	1.45	—

In the annular flow, K_L and K_G were constant at 0.05.

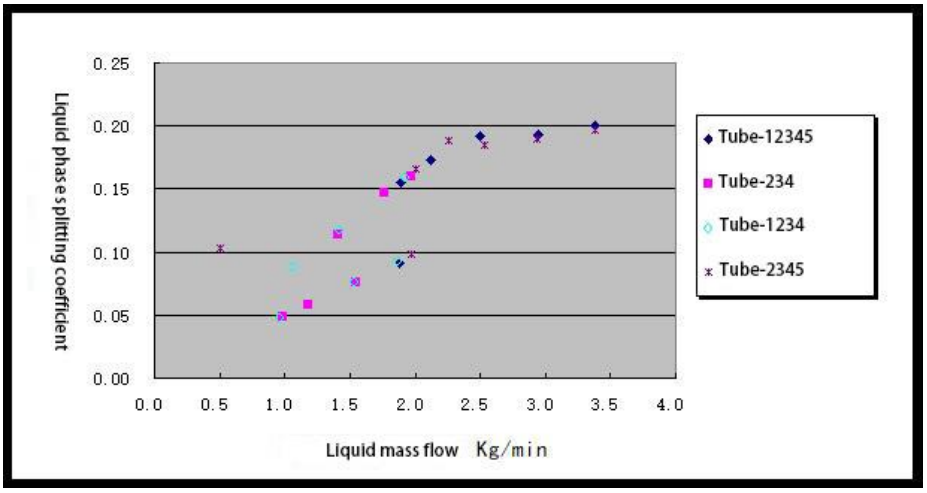

Figure 2-1a Actual measurement of liquid phase splitting coefficient under stratified flow (I)

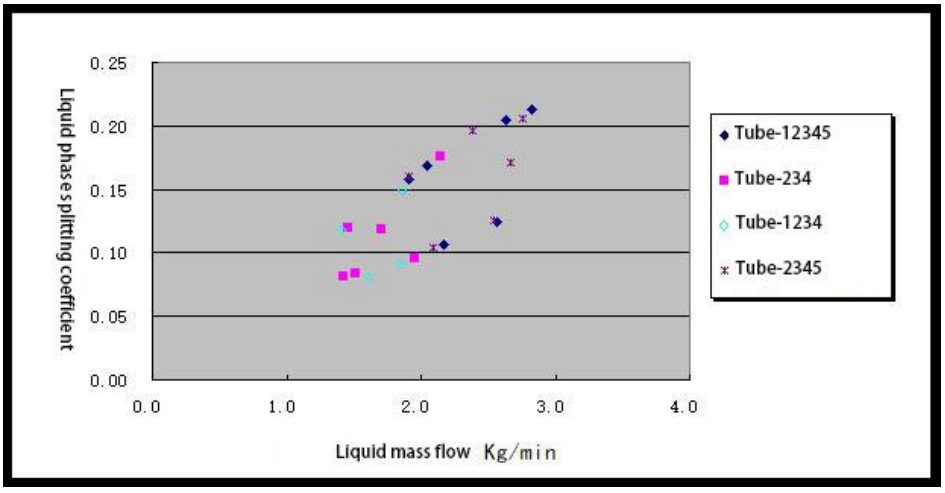

Figure 2-1b Actual measurement of liquid phase splitting coefficient under stratified flow (II)

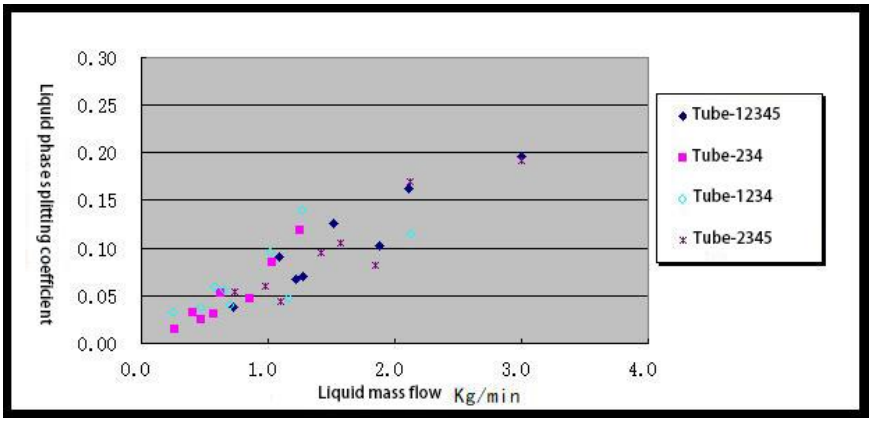

Figure 2-2a Actual measurement of liquid phase splitting coefficient under wave flow (I)

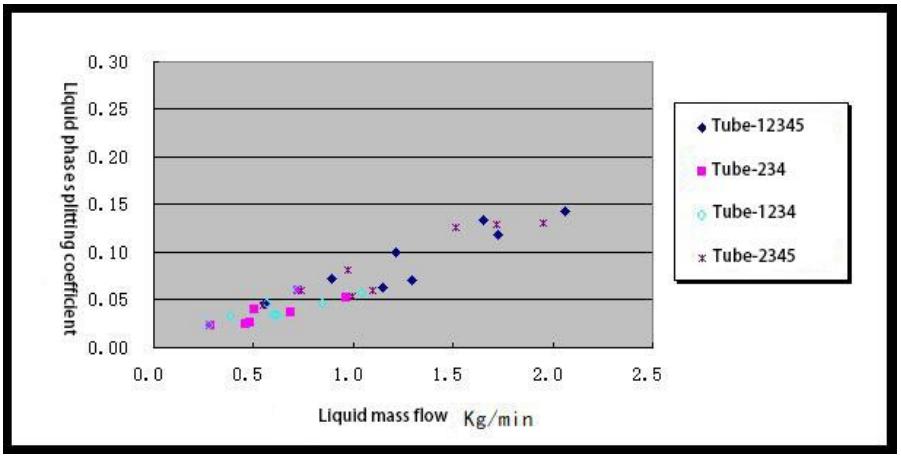

Figure 2-2b Actual measurement of liquid phase splitting coefficient under wave flow (II)

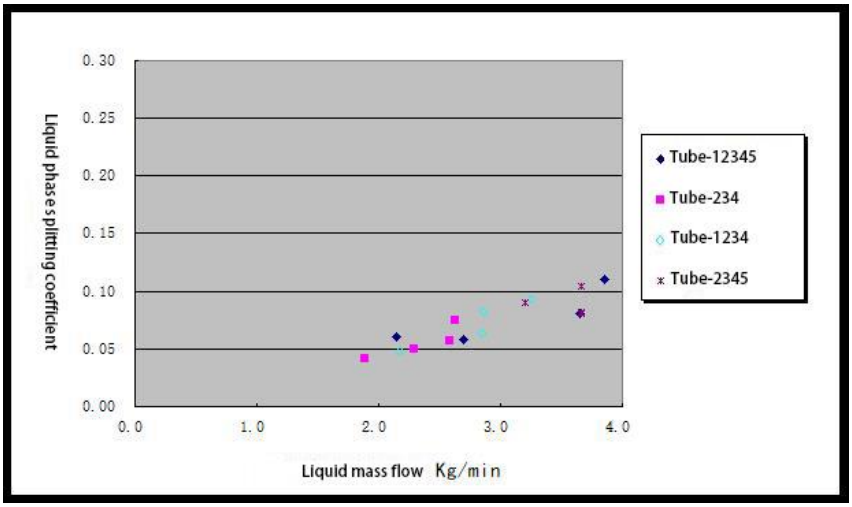

Figure 2-3a Actual measurement of liquid phase splitting coefficient under slug flow (I)

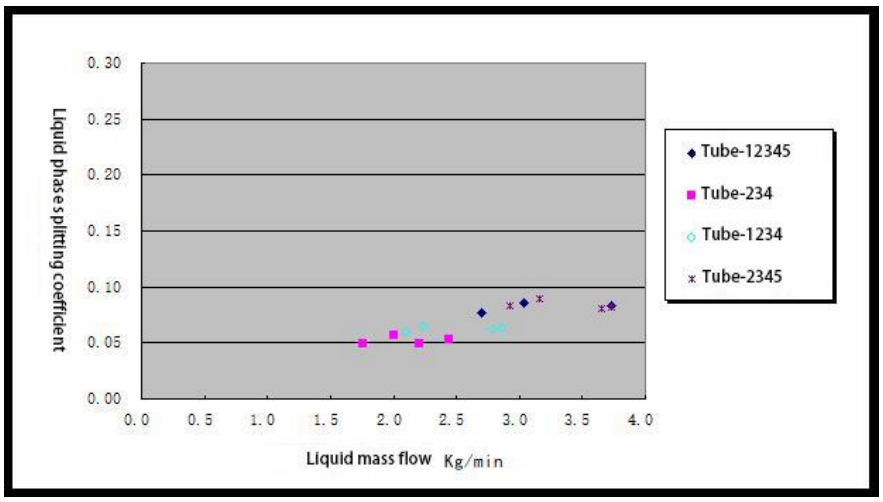

Figure 2-3b Actual measurement of liquid phase splitting coefficient under slug flow (II)

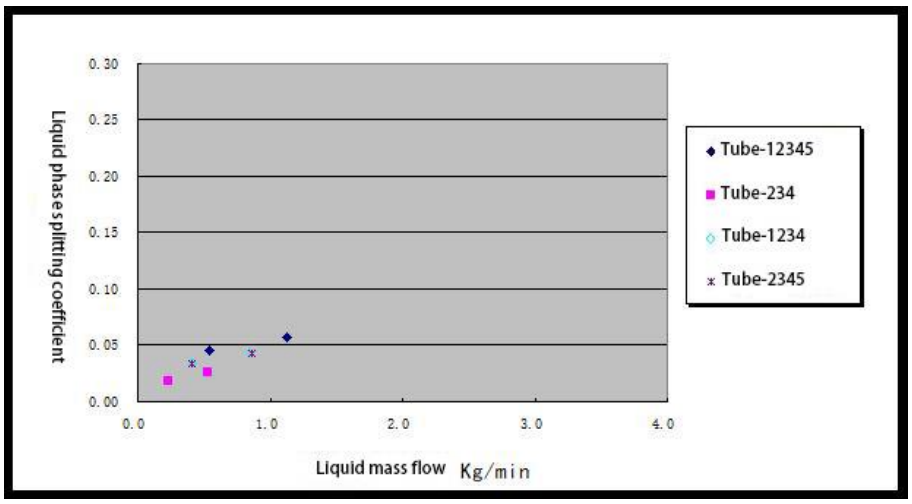

Figure 2-4a Actual measurement of liquid phase splitting coefficient under annular flow (I)

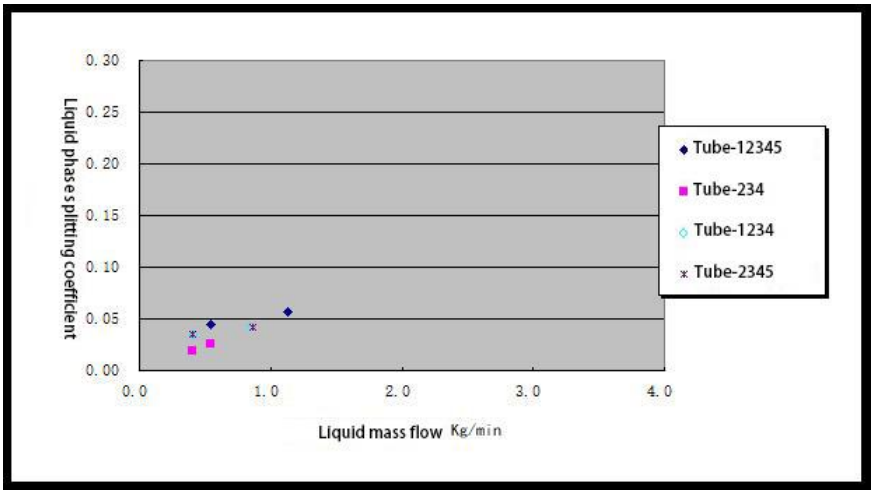

Figure 2-4b Actual measurement of liquid phase splitting coefficient under annular flow (II)

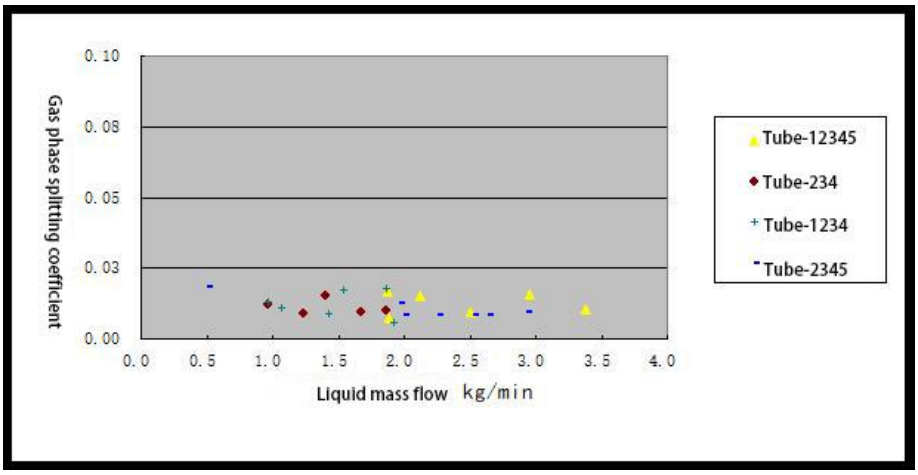

Figure 2-5a Actual measurement of gas phase splitting coefficient under stratified flow (I)

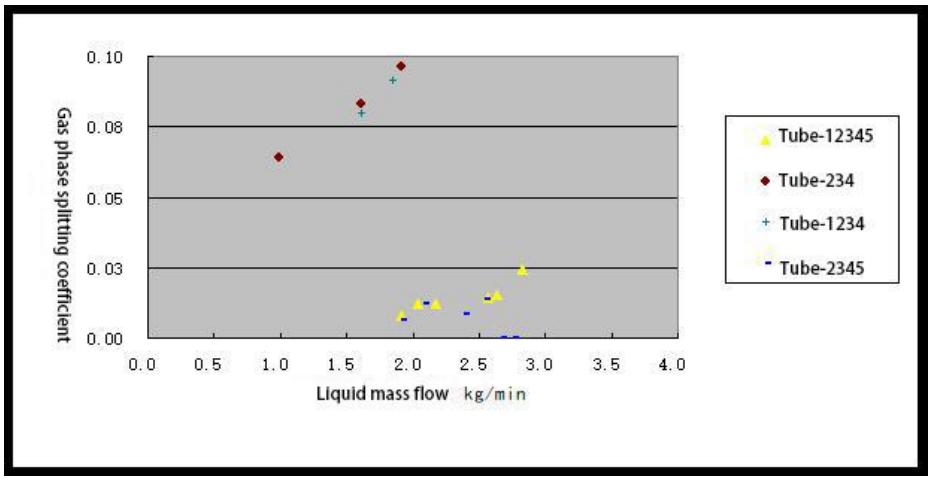

Figure 2-5b Actual measurement of gas phase splitting coefficient under stratified flow (I)

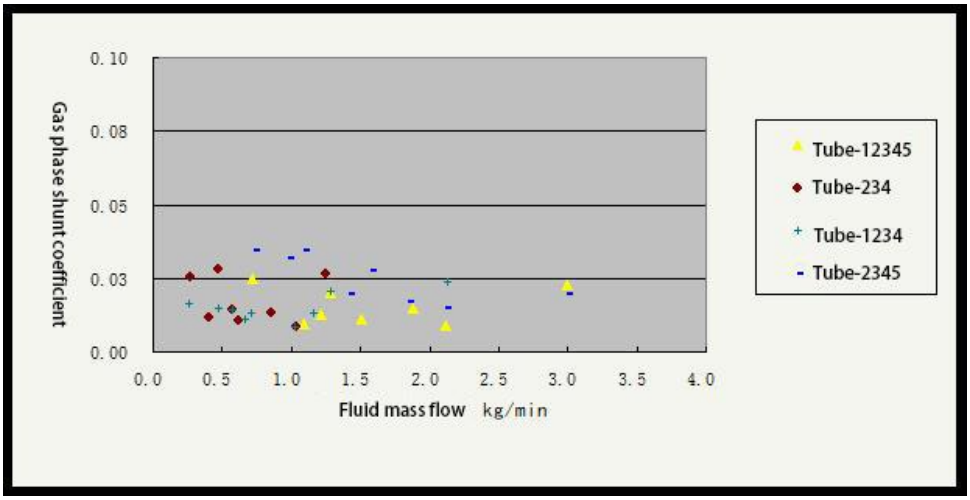

Figure 2-6a Actual measurement of gas phase shunt coefficient under wave flow (I)

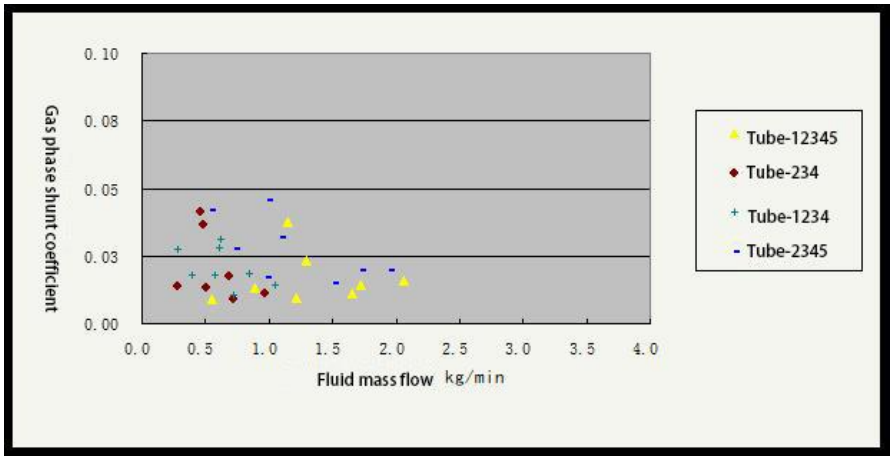

Figure 2-6b Actual measurement of gas phase shunt coefficient under wave flow (II)

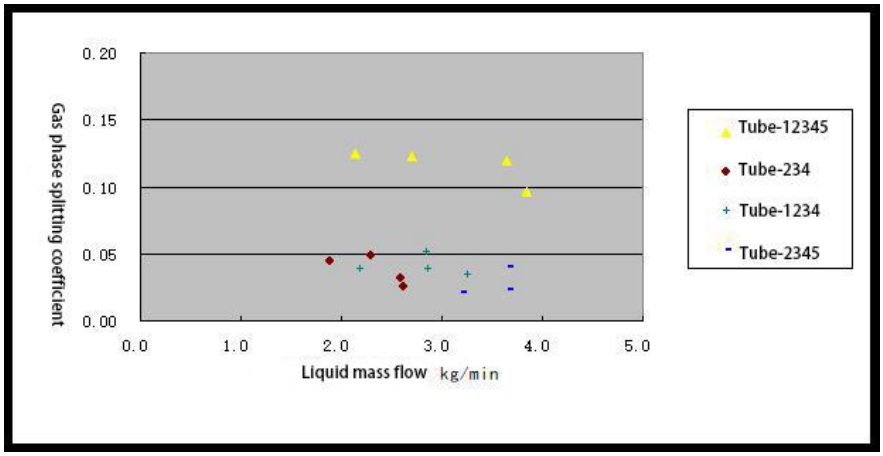

Figure 2-7a Actual measurement of gas phase splitting coefficient under slug flow (I)

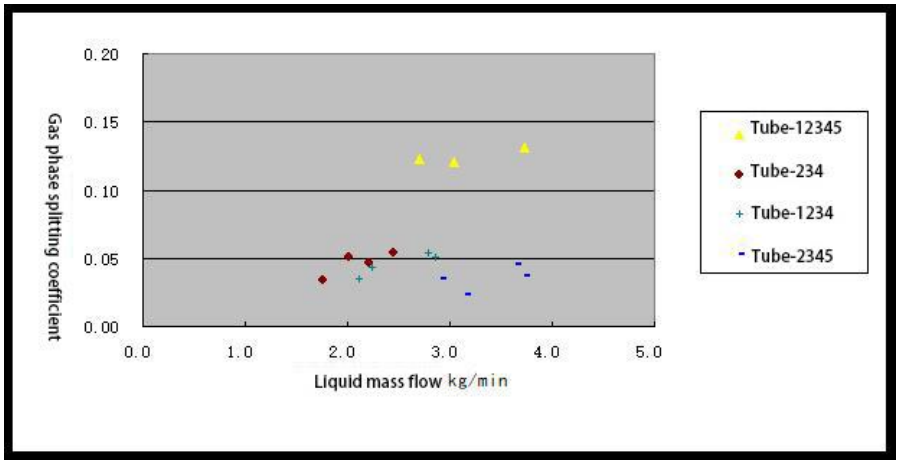

Figure 2-7b Actual measurement of gas phase splitting coefficient under slug flow (II)

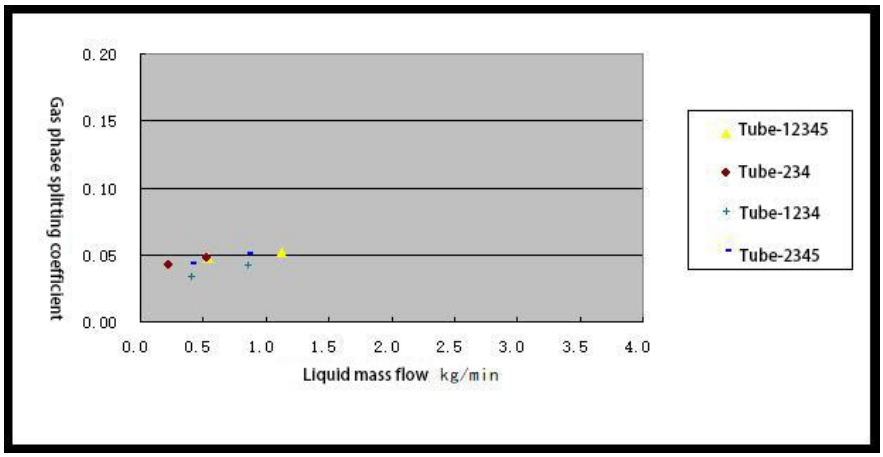

Figure 2-8a Actual measurement of gas phase splitting coefficient under annular flow (I)

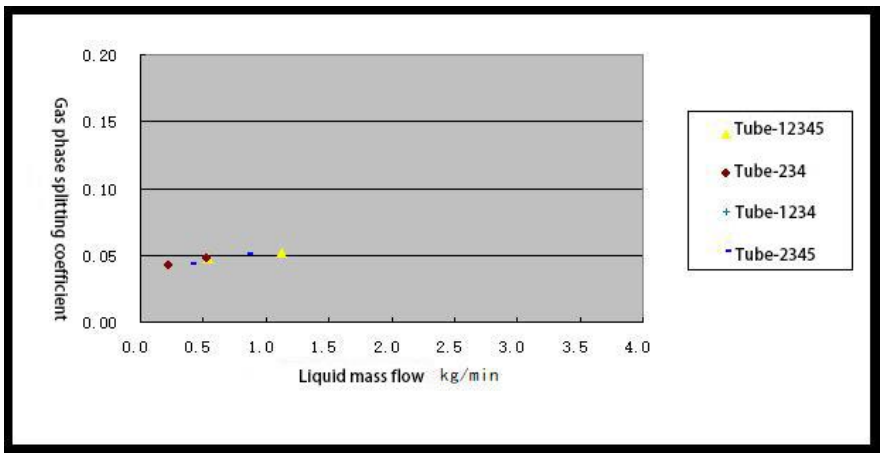

Figure 2-8b Actual measurement of gas phase splitting coefficient under annular flow (II)

2.3. Error Analysis and Conclusion

Table 2-3 Flow coefficient error analysis table

FLOW PATTERN	LIQUID PHASE SPLITTING COEFFICIENT K_L		GAS PHASE SPLITTING COEFFICIENT K_G		K_L ERROR		K_G ERROR	
	Calculated	Measured value	Calculated	Measured value	Absolute error	Standard deviation	Absolute error	Standard deviation
Laminar flow	0.182	0.198	0.0125	0.011	0.016	1.86%	0.0015	0.33%
	0.188	0.193	0.0125	0.016	0.005		0.0035	
	0.173	0.190	0.0125	0.010	0.017		—	
	0.165	0.173	0.0125	0.007	0.008		—	
	0.152	0.156	0.0125	0.015	0.004		0.0025	
	0.150	0.112	0.0125	0.016	0.038		0.0035	
Wave flow	0.168	0.185	0.0125	0.025	0.017	1.18%	0.0125	0.02%
	0.150	0.162	0.0125	0.021	0.012		0.0085	
	0.129	0.126	0.0125	0.010	0.003		—	
	0.112	0.093	0.0125	0.013	0.019		0.0005	
	0.121	0.071	0.0125	0.011	0.050		0.0015	
	0.101	0.069	0.0125	0.014	0.032		0.0015	
	0.09	0.386	0.0125	0.010	0.296		—	
Slug flow	0.073	0.087	0.125	0.125	0.014	1.08%	0.000	0.02%
	0.061	0.059	0.125	0.123	0.002		0.002	
	0.061	0.061	0.125	0.120	0.000		0.005	
	0.073	0.079	0.125	0.097	0.006		0.028	
Annular flow	0.05	0.057	0.05	0.052	0.007	0.25%	0.002	0.28%
	0.05	0.046	0.05	0.048	0.004		0.002	

Table 2-3 shows the error analysis of the liquid phase splitting coefficient and the gas phase splitting coefficient. Since the gas measurement accuracy is low in the experiment, the value of the gas phase split coefficient below 0.01 is not considered. The absolute error is the absolute value of the calculated value and the measured value difference. The standard deviation is equal to the sum of the squares of n (calculated value – measured value), then divided by (n-1), and finally squared.

$$S = \sqrt{\sum_{i=1}^{n} (x_i - x_i^{'})^2 /(n-1)} \tag{2-9}$$

3. Conclusion

Regarding the distribution characteristics of the pitot tube sampler, the following conclusions were obtained:

① The liquid phase split coefficient (K_L) is mainly affected by the position and pressure of the main section of the branch pipe. If the branch pipe is in the liquid phase concentration zone, K_L is larger; as the pressure increases, the K_L decreases, laminar and annular flow, and no effect on pressure.

② The gas phase splitting coefficient (K_G) is mainly affected by pressure. The higher the pressure, the more gas is taken. At the same time, the position of the main pipe in which the branch pipe is located also has an effect on K_G, but it is not obvious.

③ K_L decreases with the increase of liquid volume flow rate, but not the larger the flow rate, the more liquid is taken; K_G increases with the increase of liquid volume flow, but the change is not obvious.

④ Under various flow patterns, K_L gradually increases with the increase of liquid phase sampling flow rate, and finally tends to be stable.

⑤ The gas phase flow rate (gas phase conversion rate) has little effect on K_G, and its size is mainly determined by the distributor characteristics and system resistance.

References

[1] Chen Jing. Distribution characteristics of gas-liquid two-phase flow through small holes in pipe wall and its research.
[2] Wang Dong, Lin Zonghu. Separation and phase separation two-phase fluid flow measurement method [P]. Chinese Patent 98113068, 1999.9.15.
[3] Che Defu, Li Huixiong. Multiphase flow and its application.
[4] LvYuling, He Limin Overview of Multiphase Flow Measurement Technology.
[5] Rea S, Azzopardi B J. The split of horizontal stratified flow at a large diameter T-junction [J]. Chemical Engineering Research and Design, 2001, 79(4): 470-476.
[6] Mudde R F, Groen J S, Van den Akker, H E A. Two-phase flow redistribution phenomena in a large T-junction [J]. Int.J.Multiphase Flow, 1993, 19:563-573.
[7] Stacey T, Azzopardi BJ, Conte G. Split of annular two-phase flow at a small diameter T-junction [J]. Int. J. Multiphase Flow, 2000, 26(5): 845-856.
[8] Hong K C. Two-phase flow splitting at a pipe tee [J]. Journal of Petroleum Technology, 1978, 30:290-296.
[9] Seeger W. Two-phase flow in a T-jection with a horizontal inlet part I: phase separation [J].In J of Multiphase Flow, 1986, 12(4):575~585.
[10] Wang Dong, Lin Yi, Lin Zonghu. Measurement of gas flow and mass gas content of gas-liquid two-phase fluid using T-type three-way [J]. Thermal Energy Engineering, 2002, 17(4): 336-338, 348.
[11] Wang Dong, Lin Yi, Lin Zonghu. Two-phase fluid flowmeter for sample tube splitting and split phase enterprise [J] Thermal Power Engineering, 2002, 23(2): 235-237.
[12] Wang Dong, Lin Yi, Lin Zonghu. Research on flow measurement technology of gas-liquid two-phase fluid with split drum split phase [J]. Journal of Xi'an Jiaotong University, 2002, 36 (5): 4572460.
[13] Liang Fachun. Gas-liquid two-phase fluid sampler and its application in flow measurement [D]. Xi'an: School of Energy and Power Engineering, Xi'an Jiaotong University, 2006.
[14] Wang Dong, Lin Zonghu. Split-phase and split-phase two-phase fluid flowmeter [P]. China, Utility Model, ZL98251787.1999-12-04.
[15] Yang Xiaoli, Gao Wei. Overview of multiphase flow measurement techniques.
[16] Azzopardi B J. Separation at T junction [J]. Multiphase Science and Technology, 2002, 11: 223-329.
[17] Yue Wei Ting. Research on gas-liquid two-phase flow parameter detection method based on venturi [D]. Zhejiang University, 2004.
[18] Ma Huiming. Study on Flow Characteristics of Gas-liquid Reverse Spray Washing.
[19] Wang Weiwei. Study on new method for gas-liquid two-phase flow parameter detection [D] Zhejiang University, 2006.
[20] He Limin, Zhao Yuechao, Luo Xiaoming. Experimental study on the characteristic parameters of strong slug flow [J]. Journal of Engineering Thermophysics, 2005, 04
[21] Taitel Y, Barnea D. Two-phase slug flow [J]. Adv. Heat Transfer, 1990, 20:83-132.